COBEM 2023 27TH INTERNATIONAL CONGRESS OF MECHANICAL ENGENEERING

ABCM Brazilian Society of Mechanical Sciences and Engineering
27th ABCM International Congress of Mechanical Engineering
December 04-08, 2023, Florianópolis-SC, Brazil

COB-2023-1161
EFFECTIVE ELASTIC PROPERTIES OF CONCRETE BY A 3D COMPUTATIONAL HOMOGENIZATION APPROACH

Wanderson Ferreira dos Santos
Welington Hilário Vieira
Department of Structural Engineering, Sao Carlos School of Engineering, University of Sao Paulo. Address: Av. Trab. Sao Carlense, 400, Zip-Code: 13566-590, Sao Carlos, Sao Paulo, Brazil
e-mails: wanderson_santos@usp.br, wvieira@usp.br

Abstract. *This work explores a 3D computational homogenization approach to predict the effective elastic properties of concrete. The computational framework is implemented in ANSYS® Mechanical, Release 18.0 using the Ansys Parametric Design Language (APDL). In particular, the effect of heterogeneity observed at the mesoscale is modeled by the concept of Representative Volume Element (RVE), which encompasses the size distribution of aggregates inserted into the cementitious matrix. An algorithm is implemented to create coarse aggregates following a specified grading curve. Sets of 3D RVEs with different particle volumes are generated by varying the size and positions of the aggregates. Uniform strain and periodic boundary conditions are imposed on the RVEs to assess their influence on the effective constitutive behavior. The RVE models are numerically simulated using the Finite Element Method (FEM) and the effective properties are computed using average-based homogenization theory. The results for effective properties are compared with other works available in the literature, including numerical and experimental results. In summary, the homogenization strategy employed in this work provides results in close agreement with the compared studies.*

Keywords: *concrete, effective elastic properties, computational homogenization approach, heterogeneity at mesoscale, boundary conditions.*

1. INTRODUCTION

Concrete is an important building material with a wide range of applications in Civil Engineering, including the use in sidewalks, foundations, columns, beams, slabs and walls, among others structural elements. Although concrete is considered homogeneous at the macroscopic level, the lower observation scales of the material indicate a heterogeneous composition. Regarding the constituents at the mesoscale level, concrete is a composite material composed of past (mixture of cement and water) and aggregates. Consequently, the macroscpopic behavior of concrete structures depends on the geometry, spatial distribution and material properties of the individual constituents at mesoscale (Unger and Eckardt, 2011).

Methodologies for predicting the effective properties of concrete, i.e., considering the effect of heterogeneity at the mesoscale, are interesting approaches to obtain a more realistic behavior of the material at the macroscale. Some analytical estimates for the elastic modulus of heterogeneous media include the *upper bound* of Voigt (1889) and the *lower bound* of Reuss (1929). Other widely used analytical estimates in the literature were proposed by Hashin and Shtrikman (1963) based on variational principles. In the particular case of concrete, some analytical estimates were given by Counto (1964) and Hansen (1965). Analytical-experimental studies by Hirsch (1962) and Stock *et al.* (1979) are also worth mentioning. Although the previously presented analytical estimates provide closed expressions, important features are disregarded due to the complexity of the formulation with the incorporation of some variables, including the representativeness of randomness for position of inclusions with different sizes and shapes in the sample, for example. On the other hand, the increase in computer processing and the development of new algorithms stimulate the computational modeling of the behavior of concrete through numerical simulations (Chen *et al.*, 2022). Montero-Chacón *et al.* (2014) and Vorel *et al.* (2012) point out that numerical simulations allow us to conduct analyzes quickly and reduce costs with expensive tests in the laboratory. For instance, Zhou *et al.* (2014) and Li *et al.* (2019) have been focused on numerical investigations of the effective constitutive behavior for more complex samples.

In the context of computational approaches based on computational homogenization, it is worth highlighting the work developed by Wriggers and Moftah (2006) to investigate the macroscopic constitutive behavior of concrete. More specifically, Wriggers and Moftah (2006) employed a computational homogenization strategy to predict the effective properties of concrete models, taking into account the random structure of the aggregates at the mesoscopic level of the material. New algorithms were discussed for generating three-dimensional RVE models for concrete, where spherical aggregates are created from a certain aggregate size distribution. The Monte Carlo simulation method was adopted in the computational strategy to obtain effective properties with representativeness.

In particular, the present work explores a computational strategy to predict the effective elastic properties of concrete, encompassing the influence of heterogeneities observed at the mesoscale of the material in the context of 3D RVE models. In order to obtain a better representation for the distribution of aggregates in the cementitious matrix, an algorithm is implemented to define coarse aggregates following a specified grading curve, where the aggregates are created with the shape of a polyhedron. A computational homogenization approach based on numerical simulations in ANSYS® Mechanical software (Release 18.0) is adopted to obtain the homogenized properties of the material. Two boundary conditions are imposed on the RVE outer boundary: (i) the uniform strain boundary condition, and (ii) the periodic boundary condition. The effective properties computed in the present work are compared with the experimental results obtained by Stock *et al.* (1979) and the numerical results shown by Wriggers and Moftah (2006). Regarding the comparison of results, it is worth mentioning that Wriggers and Moftah (2006) considered the simplification of spherical aggregates inserted in the cementitious matrix. Furthermore, only the uniform strain boundary condition was evaluated in the computational homogenization approach adopted by Wriggers and Moftah (2006). Therefore, this study discusses the influence of aggregate morphology and the impact of the boundary condition on obtaining the effective properties of concrete.

2. 3D RVE-BASED COMPUTATIONAL HOMOGENIZATION APPROACH

In what follows, the computational homogenization approach is presented to obtain the effective elastic properties of concrete. In particular, the Ansys Parametric Design Language (APDL) is used to develop the homogenization procedure. Initially, some basic concepts of homogenization are presented, including the definition of the boundary conditions imposed to obtain the results. Afterwards, the morphologies and positions of the aggregates are defined for the RVEs, where an algorithm is implemented to create coarse aggregates following a specified grading curve. Finally, the computational procedure to obtain the effective properties from the numerical results is presented in detail.

2.1 Classical homogenization theory

In the framework of classical homogenization theories, an arbitrary point $\boldsymbol{y}$ at the macroscale (with material described as homogeneous) can be investigated with the concept of the 3D RVE, where material heterogeneity is modeled. Thus, different material models and properties can be considered to model the points $\boldsymbol{x}$ at the microscale. Some important concepts in homogenization theories are the volume average of the microscopic fields and the boundary conditions, briefly described in what follows.

2.1.1 Average-based homogenization

In the context of average-based homogenization, the macro-stress ($\boldsymbol{\Sigma}$) and macro-strain ($\boldsymbol{E}$) are defined as the volumetric averages of the micro-stress (σ) and micro-strain (ε):

$$\boldsymbol{\Sigma}\left(\boldsymbol{y}\right) = \frac{1}{V}\int_{V} \boldsymbol{\sigma}\left(\boldsymbol{x}\right) dV = \langle \boldsymbol{\sigma}\left(\boldsymbol{x}\right)\rangle, \tag{1}$$

$$\boldsymbol{E}\left(\boldsymbol{y}\right) = \frac{1}{V}\int_{V} \boldsymbol{\varepsilon}\left(\boldsymbol{x}\right) dV = \langle \boldsymbol{\varepsilon}\left(\boldsymbol{x}\right)\rangle, \tag{2}$$

where V is the total volume of the RVE.

The Hill-Mandel lemma (Bishop and Hill, 1951; Mandel, 1971) establishes the association between macroscopic and microscopic scales by an equivalence of energy in both scales:

$$\boldsymbol{\Sigma} : \boldsymbol{E} = \frac{1}{V}\int_{V} \boldsymbol{\sigma} : \varepsilon dV = \langle \boldsymbol{\sigma} : \varepsilon\rangle. \tag{3}$$

In addition, stress and strain tensors at the macroscale can be correlated by the effective stiffness tensor ($\underline{\underline{\boldsymbol{C}}}$):

$$\boldsymbol{\Sigma} = \underline{\underline{\boldsymbol{C}}} : \boldsymbol{E}, \tag{4}$$

or the effective flexibility tensor ($\underline{\underline{\boldsymbol{D}}}$):

$$\boldsymbol{E} = \underline{\underline{\boldsymbol{D}}} : \boldsymbol{\Sigma}. \tag{5}$$

2.1.2 Boundary conditions

In general, a macroscopic stress or strain field is conveniently imposed on the RVE, where a Boundary Value Problem can be solved with analytical or computational strategies. Thus, different boundary conditions can be chosen to enforce at the microscale. Two well-known boundary conditions are: (i) Uniform Strain Boundary Condition (USBC), and (ii) Periodic Boundary Condition (PBC).

The USBC results in linear displacements ($\boldsymbol{u}$) at the outer boundary of the RVE:

$$\boldsymbol{u} = \boldsymbol{E}^* \cdot \boldsymbol{x} \quad \forall \quad \boldsymbol{x} \in \partial V, \tag{6}$$

where ∂V is the nomenclature for the RVE boundary and $\boldsymbol{E}^*$ indicates the macroscale strain imposed on the RVE.

It is worth mentioning that the volume averaging of the microscopic strains results in the macroscopic strain imposed on the RVE:

$$\boldsymbol{E} = < \boldsymbol{\varepsilon} > = \boldsymbol{E}^*. \tag{7}$$

The PBC is given by:

$$\boldsymbol{u} = \boldsymbol{E}^* \cdot \boldsymbol{x} + \tilde{\boldsymbol{u}} \quad \forall \quad \boldsymbol{x} \in \partial V, \tag{8}$$

where $\tilde{\boldsymbol{u}}$ is called periodic fluctuation. It is worth mentioning that Eq. (7) is also valid for the PBC. In addition, the following expression must be checked:

$$\boldsymbol{\sigma} \cdot \boldsymbol{n}^+ = \boldsymbol{\sigma} \cdot \boldsymbol{n}^- \quad \forall \quad \boldsymbol{x} \in \partial V, \tag{9}$$

with $\boldsymbol{n}^+$ and $\boldsymbol{n}^-$ are the opposite unit normals.

Since the $\tilde{\boldsymbol{u}}$ is not known initially in the problem, the PBC is not directly imposed by Equation 8. Conveniently, an alternative is to define the RVE contour composed of positive (Γ^+) and negative parts (Γ^-), where each point $\boldsymbol{x}^+$ on Γ^+ has a corresponding point $\boldsymbol{x}^-$ on Γ^-. Thus, the displacements $\boldsymbol{u}^+$ and $\boldsymbol{u}^-$ can be written as:

$$\boldsymbol{u}^+ = \boldsymbol{E}^* \cdot \boldsymbol{x}^+ + \tilde{\boldsymbol{u}}(\boldsymbol{x}^+), \tag{10a}$$

$$\boldsymbol{u}^- = \boldsymbol{E}^* \cdot \boldsymbol{x}^- + \tilde{\boldsymbol{u}}(\boldsymbol{x}^-). \tag{10b}$$

Using the definition of periodic fluctuations on the RVE outer boundary (see Fig. 1), i.e., $\tilde{\boldsymbol{u}}\left(\boldsymbol{x}^+\right) = \tilde{\boldsymbol{u}}\left(\boldsymbol{x}^-\right)$, the PBC can be imposed by subtracting displacements of points on opposite faces ($\boldsymbol{x}^+$ and $\boldsymbol{x}^-$):

$$\boldsymbol{u}^+ - \boldsymbol{u}^- = \boldsymbol{E}^* \cdot \left(\boldsymbol{x}^+ - \boldsymbol{x}^-\right), \tag{11}$$

where the fluctuations vanish due to periodicity.

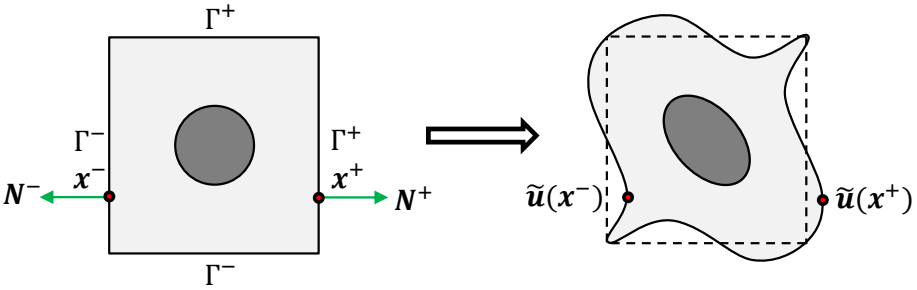

Figure 1: Illustrative scheme of an RVE with periodic fluctuations on the contour.

This strategy can be extended to 3D RVEs, where node sets must be defined for faces, edges and corners (see Fig. 2):

(i) Face nodes:

$$S_{\text{face}} = \big\{(\text{Front, Back}), (\text{Top, Bottom}), (\text{Left, Right})\big\}.$$

(ii) Edge nodes:

$$\begin{aligned} S_{\text{edge}} = \big\{&(\text{BF, CG}), (\text{BF, AE}), (\text{AE, DH}), (\text{AB, CD}), (\text{AB, EF}),\\ &(\text{EF, GH}), (\text{BC, AD}), (\text{BC, FG}), (\text{FG, EH}), (\text{AD, EH}),\\ &(\text{CD, GH}), (\text{CG, DH})\big\}. \end{aligned}$$

(iii) Corner nodes:

$$\begin{aligned} S_{\text{corner}} = \big\{&(\text{B, C}), (\text{C, G}), (\text{G, F}), (\text{A, G}), (\text{D, H}), (\text{H, E}),\\ &(\text{E, F}), (\text{B, A}), (\text{A, E}), (\text{B, F}), (\text{C, D}), (\text{G, H})\big\}. \end{aligned}$$

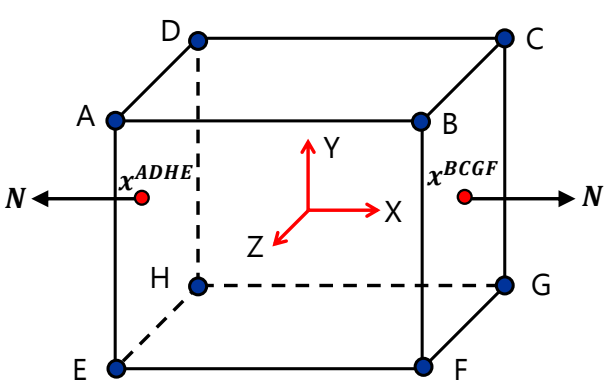

CORNERS:
A B C D E F G H
EDGES:
AB BC CD DA
EF FG GH HE
AE BF CG DH
FACES:
BCGF (FRONT)
ADHE (BACK)
ABFE (LEFT)
DCGH (RIGHT)
ABCD (TOP)
EFGH (BOTTOM)

Figure 2: Definition of sets composed of corners, edges and faces for 3D RVE.

In the particular case of finite element simulations, the mesh must be structured on the outer boundary of the RVE. Furthermore, as shown in Fig. 3, the mesh contour nodes can be divided to define the constraint equations to impose the PBC.

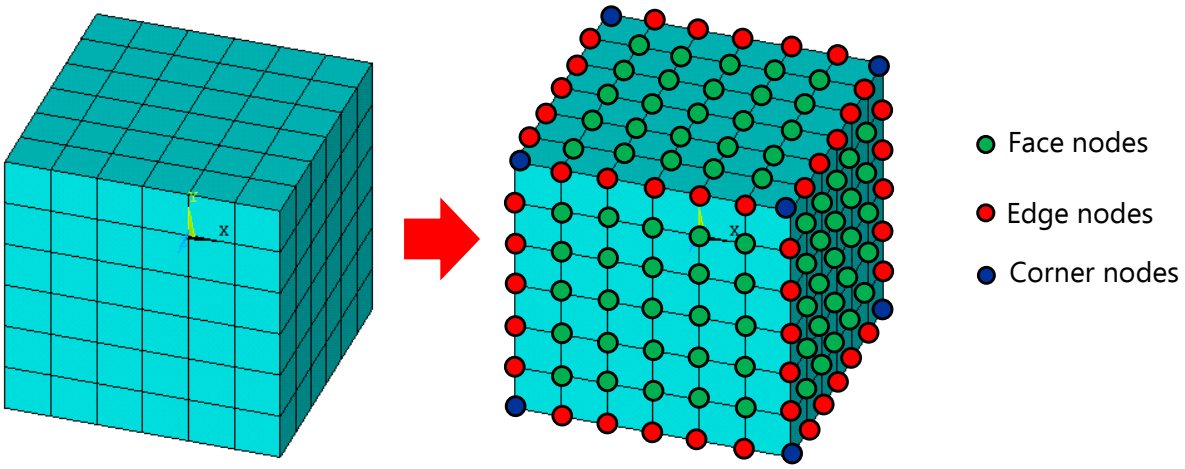

Figure 3: Definition of sets composed of corners, edges and faces for an RVE mesh (Santos, 2021).

2.2 RVE concrete models

The material behavior is considered linear elastic for the concrete. The values of Young's modulus (Y) and Poisson's coefficient (ν) for the constituents of the concrete were adopted according to Wriggers and Moftah (2006). The properties of the cementitious matrix are: $Y_m = 19$ GPa and $\nu_m = 0.2$. In turn, the aggregate properties are: $Y_a = 72$ GPa and $\nu_a = 0.2$.

Three volume fractions of aggregates (f_a) are considered in this study: (i) $f_a = 0.2$ or $f_a = 20\%$, (ii) $f_a = 0.3$ or $f_a = 30\%$, and (iii) $f_a = 0.4$ or $f_a = 40\%$ (see Fig. 5). Five aggregate distribution configurations are employed to predict the effective properties for each volume fraction of aggregates. We note that this number of realizations was sufficient to estimate the effective properties, as the variation in the results is not significant (see further details in the results and discussion).

The aggregates are generated randomly using a developed algorithm capable of producing particles in the shape of a truncated icosahedron. The truncated icosahedron is an Archimedean solid with thirty-two faces, including 12 regular pentagons and 20 regular hexagons (see Fig. 4). Although the morphology of the aggregates is close to spheres, the existence of the corners allows a more realistic modeling of coarse aggregates. According to Haäfner *et al.* (2006), considering these corners enables the consideration of stress concentrations near singular points, as seen in actual structures.

To define the dimension of each aggregate, the Fuller and Thompson (1907) curve is used to represent an ideal grading distribution for concrete. The granulometric curve for each aggregate volume fraction adopts the exponent of the Fuller and Thompson (1907) curve as 0.5, with aggregates having a maximum diameter of 19 mm and a minimum diameter of 5 mm.

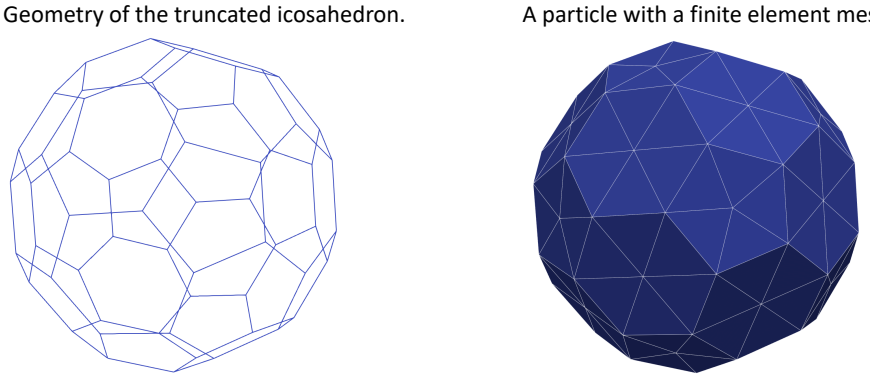

Figure 4: Polyhedron used for the representation of aggregates.

The generated aggregates are positioned using the by presented in Wriggers and Moftah (2006). Each particle is considered inscribed within a sphere that must be positioned obeying the following rules: (i) two or more aggregates cannot occupy the same space, (ii) all aggregates must be integrally within the RVE, (iii) there must be a spacing between the aggregates and between them and the edges of the sample for good quality finite element meshing (Schlangen and van Mier, 1992).

Regarding the RVE meshes, 4-node linear tetrahedrons with 3 integration points are used in the numerical simulations. For example, Fig. 6 shows the mesh of an RVE with $f_a = 0.3$, including the number of finite elements and nodes. Note that a significant amount of finite elements is required to represent three-dimensional concrete at mesoscale, since there are aggregates of small sizes.

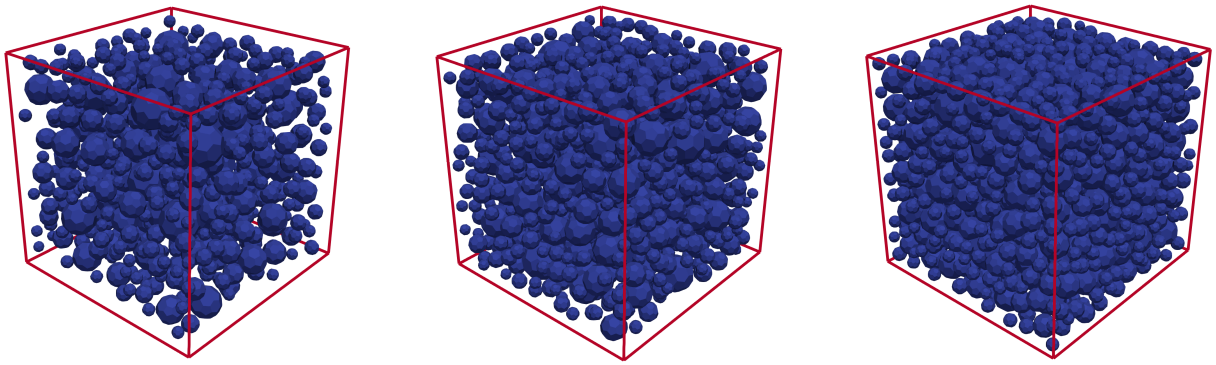

(a) RVE with $f_a = 0.2$.

(b) RVE with $f_a = 0.3$.

(c) RVE with $f_a = 0.4$.

Figure 5: RVEs with different volume fractions of aggregates (f_a)..

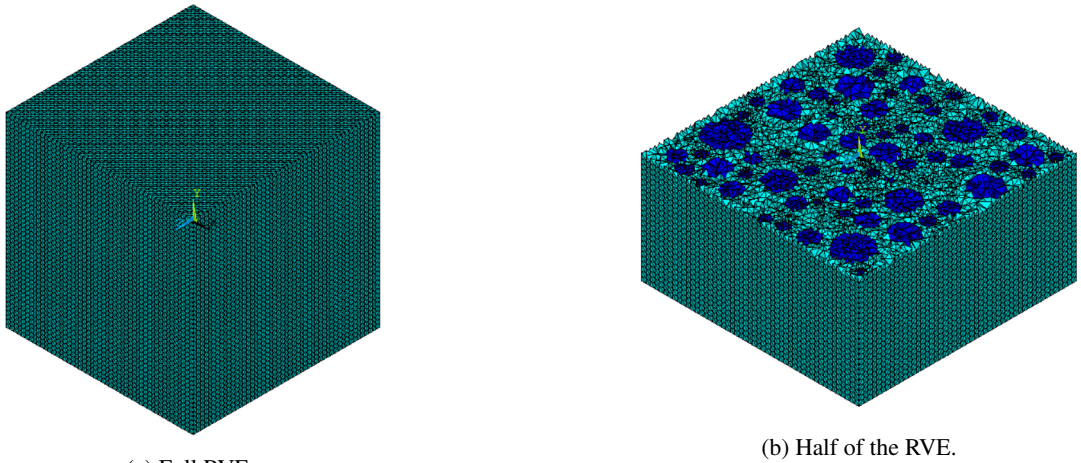

(a) Full RVE.

(b) Half of the RVE.

Figure 6: RVE with $f_a = 0.3$: 1252153 elements and 209528 nodes.

2.3 Effective elastic properties by a computational homogenization procedure in ANSYS® software

Numerical simulations with the Finite Element Method are conducted in ANSYS® Mechanical software to solve the Boundary Value Problem for the RVE, considering two boundary conditions: (i) USBC; and (ii) PBC. The language Ansys Parametric Design Language (APDL) is explored to define boundary conditions and compute the homogenized stress fields. The macroscale homogeneous strain tensor necessary to impose the boundary conditions was defined according to Wriggers and Moftah (2006):

$$\boldsymbol{E}^* = \begin{bmatrix} 0.001 & 0.001 & 0.001 \\ 0.001 & 0.001 & 0.001 \\ 0.001 & 0.001 & 0.001 \end{bmatrix}. \tag{12}$$

It is worth mentioning that the homogenized strain ($\boldsymbol{E}$) is directly obtained by the Equation 7 (i.e., $\boldsymbol{E} = \boldsymbol{E}^*$). On the other hand, in this work, the homogenized stress ($\boldsymbol{\Sigma}$) is calculated by the following expression:

$$\boldsymbol{\Sigma} = \frac{1}{V} \sum_{i=1}^{N_{\text{elem}}} \boldsymbol{\sigma}_i V_i, \tag{13}$$

where N_{elem} is the number of finite elements, $\boldsymbol{\sigma}_i$ is the average stress in the element i computed at the integration points, V_i is the volume of the element i, and V is the total volume of the RVE.

Following the approach presented by Wriggers and Moftah (2006), the effective bulk modulus (K_{ef}) is given by:

$$3K_{ef} = \frac{\text{Tr}(\boldsymbol{\Sigma})/3}{\text{Tr}(\boldsymbol{E})/3}, \tag{14}$$

and the effective shear modulus (G_{ef}) is calculated by:

$$2G_{ef} = \sqrt{\frac{\boldsymbol{\Sigma}' : \boldsymbol{\Sigma}'}{\boldsymbol{E}' : \boldsymbol{E}'}}, \tag{15}$$

where $\boldsymbol{\Sigma}'$ and $\boldsymbol{E}'$ indicate the stress and strain deviatoric tensors, respectively. Furthermore, the deviatoric tensors are computed as:

$$\boldsymbol{\Sigma}' = \boldsymbol{\Sigma} - \frac{1}{3}\,\text{Tr}(\boldsymbol{\Sigma})\boldsymbol{I}, \tag{16}$$

and

$$\boldsymbol{E}' = \boldsymbol{E} - \frac{1}{3}\,\text{Tr}(\boldsymbol{E})\boldsymbol{I}, \tag{17}$$

with $\boldsymbol{I}$ denoting the second-order identity tensor.

Finally, the effective elastic moduli or effective Young's modulus (Y_{ef}) can be obtained by:

$$Y_{ef} = \frac{9K_{ef}G_{ef}}{3K_{ef} + G_{ef}}. \tag{18}$$

3. RESULTS AND DISCUSSION

Tables 1, 2 and 3 show the effective properties of the five RVE configurations for concrete models with $f_a = 0.2$, $f_a = 0.3$ and $f_a = 0.4$, respectively. Furthermore, Tab. 4 shows the mean (M) and the standard deviation (SD) for the numerical results of the effective properties. In particular, the statistical treatment shows small differences in the results for the same f_a. The low values of SD in Table 4 indicate that employing five RVEs for each f_a is an adequate amount to predict the effective properties with sufficient representativeness.

Table 1: Numerical results of the effective properties for $f_a = 0.2$.

Sample	USBC			PBC		
	K_{ef} (GPa)	G_{ef} (GPa)	Y_{ef} (GPa)	K_{ef} (GPa)	G_{ef} (GPa)	Y_{ef} (GPa)
1	13.544	10.458	24.952	13.527	10.421	24.875
2	13.539	10.455	24.944	13.521	10.417	24.865
3	13.535	10.446	24.925	13.520	10.410	24.852
4	13.542	10.451	24.938	13.526	10.414	24.861
5	13.539	10.447	24.927	13.518	10.410	24.850

Table 2: Numerical results of the effective properties for $f_a = 0.3$.

Sample	**USBC**			**PBC**		
	K_{ef} (GPa)	G_{ef} (GPa)	Y_{ef} (GPa)	K_{ef} (GPa)	G_{ef} (GPa)	Y_{ef} (GPa)
1	15.364	11.722	28.035	15.337	11.665	27.918
2	15.370	11.729	28.051	15.342	11.671	27.931
3	15.377	11.736	28.067	15.350	11.682	27.954
4	15.391	11.748	28.095	15.364	11.691	27.976
5	15.379	11.740	28.077	15.351	11.682	27.954

Table 3: Numerical results of the effective properties for $f_a = 0.4$.

Sample	**USBC**			**PBC**		
	K_{ef} (GPa)	G_{ef} (GPa)	Y_{ef} (GPa)	K_{ef} (GPa)	G_{ef} (GPa)	Y_{ef} (GPa)
1	17.504	13.637	32.477	17.465	13.564	32.324
2	17.492	13.616	32.433	17.454	13.544	32.283
3	17.479	13.610	32.417	17.441	13.538	32.265
4	17.501	13.627	32.458	17.461	13.552	32.300
5	17.500	13.628	32.458	17.462	13.554	32.305

Table 4: Numerical results of the effective properties, inlcuding the mean (M) and the standard deviation (SD).

f_a	**Statistical parameter**	**USBC**			**PBC**		
		K_{ef} (GPa)	G_{ef} (GPa)	Y_{ef} (GPa)	K_{ef} (GPa)	G_{ef} (GPa)	Y_{ef} (GPa)
0.2	M (GPa)	13.534	10.451	24.937	13.522	10.414	24.861
	SD (GPa)	0.004	0.005	0.011	0.004	0.005	0.010
0.3	M (GPa)	15.379	11.735	28.065	15.349	11.678	27.947
	SD (GPa)	0.010	0.010	0.023	0.010	0.010	0.023
0.4	M (GPa)	17.495	13.624	32.448	17.457	13.551	32.295
	SD (GPa)	0.010	0.011	0.024	0.010	0.010	0.022

In Tab. 5, the effective properties obtained with USBC are compared to PBC. In general, the results are very close for both boundary conditions. A small increase in the relative difference was observed with the increase in the volume fraction of aggregates, but always with values smaller than 0.5%. Therefore, the boundary condition had no significant influence on the homogenized properties. In the context of simulations based on computational homogenization, the results of the boundary conditions tend to be close when the dimensions of heterogeneities are significantly smaller when compared to the dimension of the RVE (Terada *et al.*, 2000). Therefore, the results make sense due to the significantly smaller dimensions of the aggregates compared to the RVE dimension.

Table 5: Comparison of effective properties: USBC (mean) vs. PBC (mean).

f_a	**Effective elastic moduli:** Y_{ef} (GPa)		
	USBC (mean)	**PBC (mean)**	**Relative difference (%)**
	(1)	(2)	(2) to (1)
0.2	24.937	24.861	0.305%
0.3	28.065	27.947	0.420%
0.4	32.448	32.295	0.472%

Table 6 indicates the effective properties obtained with USBC compared to experimental results from Stock *et al.* (1979) (experimental results) and numerical results from Wriggers and Moftah (2006). Similarly, the comparison of results for PBC is shown in Tab. 7. The relative difference between the effective elastic modulus obtained from the presented homogenization approach and the experimental values reported by Stock *et al.* (1979) ranged from 4% to 9%. On the other hand, the relative difference in the effective elastic modulus between the presented homogenization approach and the numerical values obtained by Wriggers and Moftah (2006) ranged from 1% and 3%. Besides, the results of the

present study are closer to the experimental data when compared to the results of Wriggers and Moftah (2006). It is worth mentioning that numerical results from Wriggers and Moftah (2006) were obtained for RVEs under the USBC. Furthermore, Wriggers and Moftah (2006) considered the hypothesis of spherical aggregates in the cementitious matrix. Since the results of the present study indicated closer proximity to the experimental data, the shape for the aggregates chosen in this work (see Fig. 4) had a positive influence to the effective elastic modulus.

Table 6: Effective elastic moduli obtained with USBC (mean) compared to Stock *et al.* (1979) (experimental results) and Wriggers and Moftah (2006) (numerical results).

f_a	**Effective elastic moduli:** Y_{ef} (GPa)				
	Stock *et al.* (1979)	**Wriggers and Moftah (2006)**	**USBC (mean)**	**Relative difference (%)**	
	(1)	(2)	(3)	(3) to (1)	(3) to (2)
0.2	26.130	24.233	24.937	4.566%	2.905%
0.3	30.750	27.462	28.065	8.732%	2.196%
0.4	35.300	31.774	32.448	8.079%	2.121%

Table 7: Effective elastic moduli obtained with PBC (mean) compared to Stock *et al.* (1979) (experimental results) and Wriggers and Moftah (2006) (numerical results).

f_a	**Effective elastic moduli:** Y_{ef} (GPa)				
	Stock *et al.* (1979)	**Wriggers and Moftah (2006)**	**PBC (mean)**	**Relative difference (%)**	
	(1)	(2)	(3)	(3) to (1)	(3) to (2)
0.2	26.130	24.233	24.861	4.856%	2.592%
0.3	30.750	27.462	27.947	9.115%	1.766%
0.4	35.300	31.774	32.295	8.513%	1.640%

The conclusions are similar for both boundary conditions investigated in this work. The results obtained in the present work are in close agreement with the numerical results of Wriggers and Moftah (2006), in which more sensitive differences are noted for $f_a = 0.2$. On the other hand, more significant differences are observed when numerical results from USBC and PBC are compared with experimental data from Stock *et al.* (1979).

4. CONCLUSIONS

In this work, a computational homogenization procedure was explored to predict the effective elastic properties of concrete. The computational homogenization procedure was implemented in the ANSYS® Mechanical software (Release 18.0) using the Ansys Parametric Design Language (APDL). The uniform strain boundary condition and the periodic boundary condition were imposed on the RVEs in the context of three-dimensional numerical simulations. An algorithm was used to generate RVEs with the representation of inclusions at mesoscale following a specific granulometric curve.

In summary, the comparison between USBC and PBC indicated close results for the effective modulus of elasticity. Thus, the boundary condition did not significantly influence the results. Furthermore, the results obtained with the computational homogenization procedure were close to the experimental and numerical data compared in the discussion of the results. In future works, we intend to investigate more realistic geometries for the aggregates inserted in the cementitious matrix. Finally, the proposed approach is interesting to investigate the effective macroscopic behavior of composite materials, encompassing the possibility of modeling characteristics of the constituents such as varied volume fractions, influence of the geometry and distribution of inclusions and different constitutive properties, for example.

5. ACKNOWLEDGEMENTS

The authors would like to gratefully acknowledge Conselho Nacional de Desenvolvimento Científico e Tecnológico - Brasil (CNPq) and Coordenação de Aperfeiçoamento de Pessoal de Nível Superior (CAPES) for the research grants.

6. REFERENCES

Bishop, J.F.W. and Hill, R., 1951. "Xlvi. a theory of the plastic distortion of a polycrystalline aggregate under combined stresses". *The London, Edinburgh, and Dublin Philosophical Magazine and Journal of Science*, Vol. 42, pp. 414–427.

Chen, P., Liu, J., Cui, X. and Si, S., 2022. "Mesoscale analysis of concrete under axial compression". *Construction and Building Materials*, Vol. 337, p. 127580.

Counto, U.J., 1964. "The effect of the elastic modulus of the aggregate on the elastic modulus, creep and creep recovery of concrete". *Magazine of Concrete Research*, Vol. 16, pp. 129–138.

Fuller, W.B. and Thompson, S.E., 1907. "The laws of proportioning concrete". *Transactions of the American Society of Civil Engineers*, Vol. 59, No. 2, pp. 67–143.

Haäfner, S., Eckardt, S., Luther, T. and Könke, C., 2006. "Mesoscale modeling of concrete: Geometry and numerics". *Computers and Structures*, Vol. 84, pp. 450–461.

Hansen, T.C., 1965. "Influence of aggregate and voids on modulus of elasticity of concrete, cement mortar, and cement paste". Vol. 62.

Hashin, Z. and Shtrikman, S., 1963. "A variational approach to the theory of the elastic behaviour of multiphase materials". *Journal of the Mechanics and Physics of Solids*, Vol. 11, pp. 127–140.

Hirsch, T.J., 1962. "Modulus of elasticity iof concrete affected by elastic moduli of cement paste matrix and aggregate". Vol. 59.

Li, K.Q., Li, D.Q., Li, P.T. and Liu, Y., 2019. "Meso-mechanical investigations on the overall elastic properties of multi-phase construction materials using finite element method". *Construction and Building Materials*, Vol. 228, p. 116727.

Mandel, J., 1971. *Plasticité classique et viscoplasticité*. Springer-Verlag, Udine, Italy.

Montero-Chacón, F., Marín-Montín, J. and Medina, F., 2014. "Mesomechanical characterization of porosity in cementitious composites by means of a voxel-based finite element model". *Computational Materials Science*, Vol. 90, pp. 157–170.

Reuss, A., 1929. "Berechnung der fließgrenze von mischkristallen auf grund der plastizitätsbedingung für einkristalle ." *ZAMM - Journal of Applied Mathematics and Mechanics / Zeitschrift für Angewandte Mathematik und Mechanik*, Vol. 9, pp. 49–58.

Santos, W.F., 2021. *Computational modeling of the rupture of elasto-plastic media with initial voids*. Master's degree in civil engineering (structural engineering), São Carlos School of Engineering, University of São Paulo, São Carlos.

Schlangen, E. and van Mier, J.G.M., 1992. "Simple lattice model for numerical simulation of fracture of concrete materials and structures". *Materials and Structures*, Vol. 25, pp. 534–542.

Stock, A.F., Hannantt, D.J. and Williams, R.I.T., 1979. "The effect of aggregate concentration upon the strength and modulus of elasticity of concrete". *Magazine of Concrete Research*, Vol. 31, pp. 225–234. doi: 10.1680/macr.1979.31.109.225.

Terada, K., Hori, M., Kyoya, T. and Kikuchi, N., 2000. "Simulation of the multi-scale convergence in computational homogenization approaches". *International Journal of Solids and Structures*, Vol. 37, No. 16, pp. 2285–2311.

Unger, J.F. and Eckardt, S., 2011. "Multiscale modeling of concrete". *Archives of Computational Methods in Engineering*, Vol. 18, pp. 341–393.

Voigt, W., 1889. "Ueber die beziehung zwischen den beiden elasticitätsconstanten isotroper körper". *Annalen der Physik*, Vol. 274, pp. 573–587.

Vorel, J., Šmilauer, V. and Bittnar, Z., 2012. "Multiscale simulations of concrete mechanical tests". *Journal of Computational and Applied Mathematics*, Vol. 236, No. 18, pp. 4882–4892.

Wriggers, P. and Moftah, S., 2006. "Mesoscale models for concrete: Homogenisation and damage behaviour". *Finite Elements in Analysis and Design*, Vol. 42, No. 7, pp. 623–636. The Seventeenth Annual Robert J. Melosh Competition.

Zhou, C., Li, K. and Ma, F., 2014. "Numerical and statistical analysis of elastic modulus of concrete as a three-phase heterogeneous composite". *Computers & Structures*, Vol. 139, pp. 33–42.

7. RESPONSIBILITY NOTICE

The authors are solely responsible for the printed material included in this paper.